Published in "The Plant Journal 95 (2): 187–203, 2018"
which should be cited to refer to this work.

A conserved RxLR effector interacts with host RABA-type GTPases to inhibit vesicle-mediated secretion of antimicrobial proteins

Iga Tomczynska, Michael Stumpe and Felix Mauch*
Department of Biology, University of Fribourg, chemin du musée 10, 1700, Fribourg, Switzerland

*For correspondence (e-mail felix.mauch@unifr.ch).

SUMMARY

Plant pathogens of the oomycete genus Phytophthora produce virulence factors, known as RxLR effector proteins that are transferred into host cells to suppress disease resistance. Here, we analyse the function of the highly conserved RxLR24 effector of *Phytophthora brassicae*. RxLR24 was expressed early in the interaction with Arabidopsis plants and ectopic expression in the host enhanced leaf colonization and zoosporangia formation. Co-immunoprecipitation (Co-IP) experiments followed by mass spectrometry identified different members of the RABA GTPase family as putative RxLR24 targets. Physical interaction of RxLR24 or its homologue from the potato pathogen *Phytophthora infestans* with different RABA GTPases of Arabidopsis or potato, respectively, was confirmed by reciprocal Co-IP. In line with the function of RABA GTPases in vesicular secretion, RxLR24 co-localized with RABA1a to vesicles and the plasma membrane. The effect of RxLR24 on the secretory process was analysed with fusion constructs of secreted antimicrobial proteins with a pH-sensitive GFP tag. PATHOGENESIS RELATED PROTEIN 1 (PR-1) and DEFENSIN (PDF1.2) were efficiently exported in control tissue, whereas in the presence of RxLR24 they both accumulated in the endoplasmic reticulum. Together our results imply a virulence function of RxLR24 effectors as inhibitors of RABA GTPase-mediated vesicular secretion of antimicrobial PR-1, PDF1.2 and possibly other defence-related compounds.

Keywords: Phytophthora, RxLR effector, RABA GTPases, secretion, plant immunity, *Arabidopsis thaliana*, *Solanum tuberosum*.

INTRODUCTION

Plants have evolved an innate immune system comparable to innate immunity of animals (Jones and Dangl, 2006; Dodds and Rathjen, 2010). Plasma membrane localized pattern recognition receptors (PRRs) monitor the extracellular environment for molecules of microbial origin (pathogen-associated molecular patterns; Zipfel, 2014). Activated PRRs initiate pattern-triggered immunity (PTI) that provides a broad level of basic disease resistance to a wide variety of microbes (Boller and Felix, 2009). To counteract the negative effects of PTI, pathogens evolved effector molecules that are delivered into the host to interfere with defense responses or alter plant metabolism to the advantage of the pathogen. Effectors include low-molecular-weight compounds as well as proteins that are either delivered to the host apoplast or into host cells (Rafiqi *et al.*, 2012; Le Fevre *et al.*, 2015). In turn, plants evolved a second class of intracellular immune receptors in the form of disease resistance proteins that can recognize the presence of effectors and initiate effector-triggered immunity (Jones and Dangl, 2006; Takken and Tameling, 2009).

The ultimate immune reactions interfering with pathogen progress include cytological and biochemical changes (Chisholm *et al.*, 2006). Plants cells can initiate local apoptotic cell death at the site of pathogen attack or strengthen the cell walls via deposition of the glucan polymer callose to prevent pathogen entry. Important components of biochemical defences include enhanced production of reactive oxygen species and a variety of antimicrobial molecules. The initial interactions between pathogen and host plant take place at the plant surface and in the apoplast where filamentous pathogens such as fungi and oomycetes extend their hyphae into the intercellular space.

Consequentially, plants secrete in response to pathogens many antagonistic compounds, such as hydrolytic enzymes, enzyme inhibitors, and antimicrobial proteins and metabolites. Vesicle-mediated exocytosis is also responsible for the delivery to the plasma membrane of other immunity-related compounds, such as PRRs, callose synthase and NADPH oxidases that are involved in the generation of reactive oxygen species (Frei dit Frey and Robatzek, 2009; Inada and Ueda, 2014; Wang *et al.*, 2016). Functioning secretory pathways were shown to be essential for disease resistance (Wang *et al.*, 2005; Kwon *et al.*, 2008; Du *et al.*, 2018).

The involvement of vesicular trafficking in the targeting and delivery of many immune-relevant compounds makes the secretory process an attractive target for pathogen effectors. Effectors from *Pseudomonas syringae*, powdery mildew and *Phytophthora infestans*, respectively, were shown to directly interact with components of the secretory machinery (Nomura *et al.*, 2006; Schmidt *et al.*, 2014; Du *et al.*, 2015).

The oomycete genus Phytophthora contains more than 120 species, including some of the most devastating plant pathogens (http://www.phytophthoradb.org/species.php). For example, *P. infestans* causes the late blight disease of potato and tomato that is considered as a serious threat to food security (Haas *et al.*, 2009; Cooke *et al.*, 2012). Diseases caused by Phytophthora species generate not only substantial economic losses, estimated at €5.2 billion per year for the late blight disease alone (Haverkort *et al.*, 2009), but also can threaten woodlands as seen in forest diebacks (Anderson *et al.*, 2010).

The success of Phytophthora as a pathogen depends on its complement of effector proteins. Genome analysis revealed the presence of hundreds of different effectors in individual Phytophthora species (Tyler *et al.*, 2006; Haas *et al.*, 2009). By far the largest group is defined by a conserved Arg-any amino acid-Leu-Arg (RxLR) sequence motif, which is located about 30 amino acids downstream of the signal peptide and often is followed by a dEER (Asp-Glu-Glu-Arg) motif (Whisson *et al.*, 2007; Dou *et al.*, 2008). Effector delivery depends on the presence of the RxLR sequence motif, but the mechanism of translocation into host cells is still under debate (Dou *et al.*, 2008; Ellis and Dodds, 2011; Kale, 2012; Wawra *et al.*, 2013; Yaeno and Shirasu, 2013). The C-terminal sequences of RxLR effectors comprising the actual effector function rarely contain motifs that would suggest a known biochemical function. Many RxLR effectors have been shown to compromise disease resistance when expressed directly in plants, and some of their targets have been identified. These targets are very diverse, and include the host ubiquitin E3 ligase CMPG1 (Bos *et al.*, 2010), the lectin receptor kinase LecRK-I.9 (Bouwmeester *et al.*, 2011), the phosphatase BSL1 (Saunders *et al.*, 2012), NAC transcription factors (McLellan *et al.*, 2013), MAPKKK epsilon (King *et al.*, 2014), a component of small RNA pathway (Qiao *et al.*, 2015), DYNAMIN-RELATED PROTEIN 2 (Chaparro-Garcia *et al.*, 2015), RNA binding protein StKRBP1 (Wang *et al.*, 2015), PROTEIN PHOSPHATASE TYPE 1C (Boevink *et al.*, 2016), EXOCYST COMPONENT SEC5 (Du *et al.*, 2015), NPH3/RPT2-Like Protein StNRL1 (Yang *et al.*, 2016); autophagy cargo receptor ATG8CL (Dagdas *et al.*, 2016), and endoplasmic reticulum (ER)-luminal binding immunoglobulin proteins (Jing *et al.*, 2016).

Here, we focus on the functional characterization of the RxLR effector 24 (RxLR24) of *Phytophthora brassicae* (*P. brassicae*) with unusual high sequence conservation across Phytophthora species. RxLR24 is expressed during the infection process of Arabidopsis, and is active as a virulence factor as *in planta* expression enhanced disease susceptibility towards *P. brassicae*. We show that RxLR24 of *P. brassicae*, a pathogen of *Arabidopsis thaliana*, and the corresponding homologue of *P. infestans* physically interact with various RABA GTPases to inhibit host vesicular trafficking and interfere with the secretion of antimicrobial compounds.

RESULTS

Characterization of an evolutionary conserved Phytophthora RxLR effector

We were interested in highly conserved RxLR effectors as sequence conservation argues for a conserved function of effector homologues in different hosts. Here, we focus on the *P. brassicae* effector RxLR24 (*Pb*RxLR24) and its homologue of *P. infestans* (*Pi*RxLR24). *PbRxLR24* encodes a protein of 155 amino acids with a molecular mass of 17.7 kDa. It contains a predicted 21-amino-acid-long N-terminal signal peptide followed by an RxLR-dEER motif starting at position 52 and a putative functional C-terminal domain. *Pb*RxLR24 shares extensive sequence identity with homologues of other Phytophthora species (Figure S1; Table S1). *Pi*RxLR24, for example, shares 51% sequence identity (65% similarity) with *Pb*RxLR24.

RxLR24 is expressed by *Phytophthora brassicae* during infection

To explore the possible contribution of *Pb*RxLR24 to *P. brassicae* virulence, transcript levels at different infection stages were analysed by quantitative polymerase chain reaction (qPCR). The susceptible Arabidopsis mutant *cyp79B2 cyp79B3* was inoculated with zoospores of *P. brassicae* isolate CBS 179.87 (Schlaeppi *et al.*, 2010). *PbRxLR24* transcripts were present in the zoospores, and their relative expression level with regard to *ß-tubulin* and *actin* transcripts of *P. brassicae* increased during the infection process to reach a maximum of 12-fold induction at 96 hpi (Figure S2).

Analysis of transgenic Arabidopsis with ectopic expression of *Pb*RxLR24

To learn more about the function of *Pb*RxLR24, Arabidopsis plants of the accession Wassilewskija (Ws-0) were

transformed with two different constructs expressed under the control of the CaMV-35S promoter. In the first RxLR24 fusion protein the signal peptide was replaced with a 3xFLAG tag (FLAG-RxLR24), and in the second one with a GFP tag (GFP-RxLR24). Interestingly, *in planta* expression of RxLR24 lead in some lines to developmental abnormalities in the form of severely reduced growth (Figure 1a), suggesting interference of RxLR24 with house-keeping processes. Analysis of *RxLR24* transcript abundance with qPCR (Figure 1b) and protein abundance with immunoblots (Figure 1c) revealed a correlation between the *RxLR24* expression level and reduced plant growth. Highest *RxLR24* transcript levels were present in the severely dwarfed homozygous Arabidopsis lines L3, L4 and L5. Medium levels were found in plants with small growth retardation (hemizygous lines L3, L4 and L5), whereas plants with low expression level showed a wild-type (WT) phenotype (homozygous L1 and L2 lines). This correlation was also reflected at the protein level.

RxLR24 contributes to pathogen virulence

The test for disease resistance of the RxLR24 expressing Arabidopsis lines was restricted to low and medium expression lines as the growth phenotype excluded the high expression lines from meaningful analysis. After leaf inoculation with a zoospore suspension of *P. brassicae* (CBS 179.87), the disease phenotype was scored 7 dpi based on symptom development and zoosporangia production (Figure 2). Inoculation of WT plants caused symptoms limited to a few brown necrotic lesions (Figure 2a). The RxLR24 lines showed extended lesions that remained within the area of the inoculation droplet in low expression lines (lines L1 and L2) and did outgrow this area in medium expression lines (hemizygous lines L3, L4, L5). Quantitative analysis based on resistance scores on a scale of 0–4 (0 = fully susceptible; 4 = fully resistant; Schlaeppi *et al.*, 2010) confirmed statistically significant differences between WT, the low and the medium expression lines (Figure 2b). RxLR24 influenced the capacity for asexual reproduction. *Phytophthora brassicae* could not proliferate in WT plants beyond small lesions at the infection site, whereas it colonized the leaf tissue of RxLR24 lines to reproduce in the form of zoosporangia (Figure 2c). Quantitative analysis detected no zoosporangia in WT plants, whereas up to 35% of the leaves of RxLR24 lines contained zoosporangia (Figure 2d). The expression level of RxLR24 correlated with the level of zoosporangia production. In summary, ectopic expression of RxLR24 in Arabidopsis enhanced the virulence of the hemibiotrophic oomycete *P. brassicae*, indicating that RxLR24 is a functional virulence factor with a putative immunity-related target in Arabidopsis. In contrast, the ectopic expression of RxLR24 did not affect the virulence of the necrotrophic fungal pathogen *Botrytis cinerea* (Figure S3).

RxLR24 homologues of *Phytophthora brassicae* and *Phytophthora infestans* specifically associate with members of the RABA GTPase subfamily

In planta co-immunoprecipitation (Co-IP) followed by liquid chromatography-tandem mass spectrometry (LC-MS/MS) was applied to identify putative host targets of *Pb*RxLR24. The FLAG-RxLR24 fusion protein was immunoprecipitated from extracts of transgenic Arabidopsis with magnetic beads coated with anti-FLAG antibody. Mass spectrometry identified 12 Arabidopsis proteins that appeared to specifically associate with RxLR24 in the immunoprecipitate compared with negative controls consisting of three unrelated FLAG-RxLR fusion proteins (Table S2). The top 11 proteins represented members of the RABA GTPase subfamily, followed by RABG3f and two chloroplast proteins. The last two candidates were excluded from further analysis as respective peptides were also identified in the immunoprecipitate of the negative controls. A list of peptides identified in the Co-IP of RxLR24 is shown in File S1. Reciprocal Co-IP was performed to further test the specificity of the interaction between RAB GTPases and *Pb*RxLR24. Candidates from different subfamilies, RABA1a, RABA2a and RABA4a, and RABG3f were individually co-expressed as Myc-tagged fusion protein in agro-infiltrated *Nicotiana benthamiana* leaves together with FLAG-RxLR24. The Myc-tagged RAB proteins were immunoprecipitated with anti-Myc antibody-coated agarose beads and the precipitate was tested for the presence of FLAG-tagged *Pb*RxLR24 (Figure 3a). The results showed that the Myc-antibody did not directly precipitate the FLAG-RxLR24 protein. RxLR24 did not Co-IP with RABG3f, whereas it was present in the Co-IPs of all three tested RABA proteins, confirming physical interaction between *Pb*RxLR24 and RABA proteins. Similar Co-IP experiments were performed to test the interaction of *Pi*RxLR24 of *P. infestans* with three RABA proteins of potato. To this end a FLAG-*Pi*RxLR24 fusion protein and Myc-tagged potato homologues of RABA1a, RABA2a and RABA4a were transiently expressed in *N. benthamiana* leaves, and immunoprecipitation was performed with anti-Myc antibody-coated agarose beads. *Pi*RxLR24 was not directly precipitated by the anti-Myc antibody, whereas it was pulled down in the presence of any of the three Myc-tagged potato RABA proteins (Figure 3b). Together, our results support the conclusion that RxLR24 proteins of *P. brassicae* and *P. infestans* interact with RABA GTPases of the respective host species.

RxLR24 co-localizes with RABA proteins

The subcellular distribution of *Pb*RxLR24 was analysed by confocal microscopy in leaves of *N. benthamiana* that transiently expressed the GFP-RxLR24 fusion construct (Figure 4). GFP-RxLR24 localized to a continuous layer at the cell periphery and to mobile dot-like structures (Figure 4a,

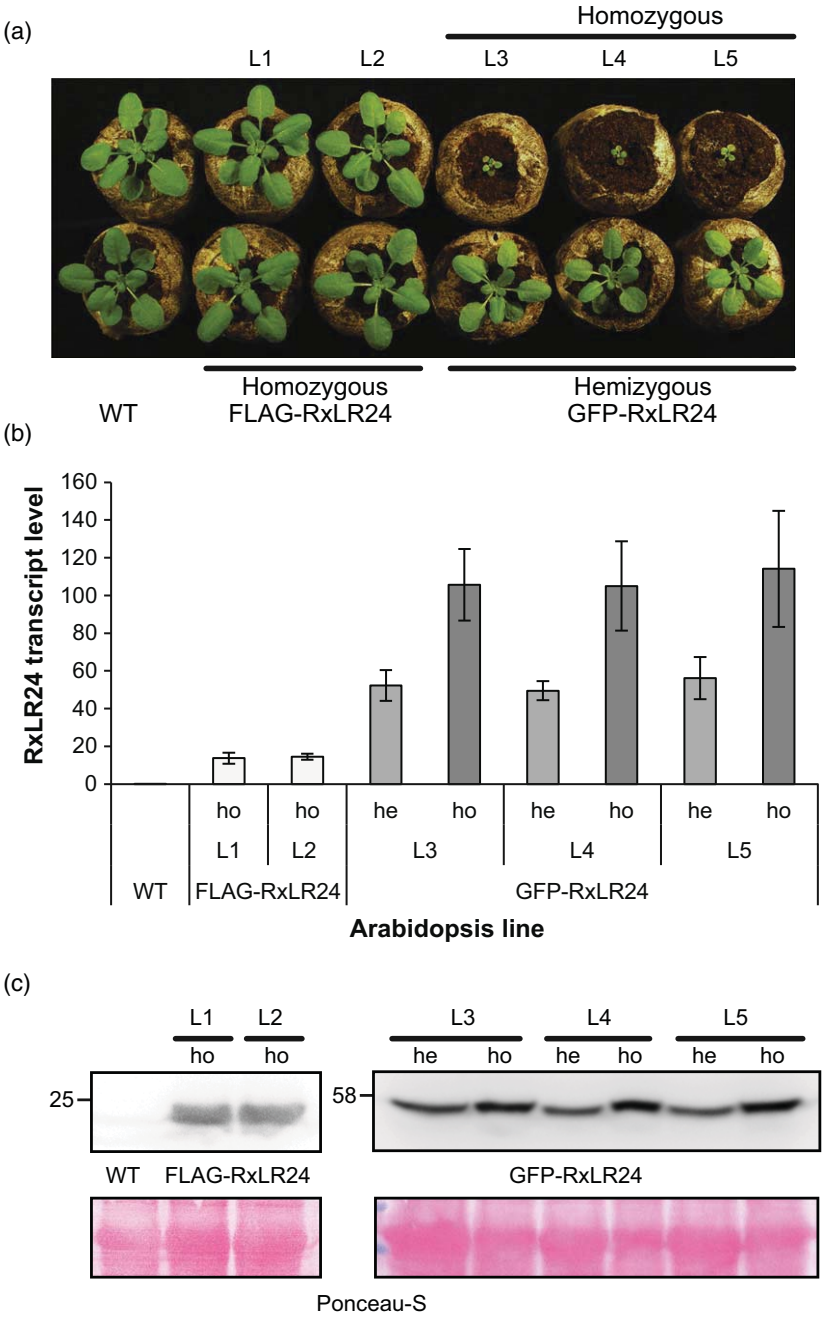

Figure 1. Characterization of Arabidopsis *Pb*RxLR24 over-expression lines.
(a) Comparison of growth phenotype of the Arabidopsis wild-type (WT) accession Ws-0 with five independent lines constitutively expressing either FLAG- or GFP-tagged RxLR24.
(b) Relative *PbRxLR24* transcript abundance compared with transcripts of *expG* as reference gene (Czechowski *et al.*, 2005) in WT and RxLR24 expressing homozygous (ho) and hemizygous (he) lines. Results represent the mean values (± SD) of two experiments.
(c) Immunoblot analysis of RxLR24 protein accumulation in WT and different RxLR24 expressing lines. Blots were developed with FLAG- and GFP-specific antibodies, respectively. Ponceau-S (PS)-stained Rubisco large subunit served as a loading control.

left; Movies S1 and S2). Deletion of the C-terminus of RxLR24 in RxLR24ΔC changed the localization of GFP fluorescence to the cytoplasm and nucleus (Figure 4a, right). The GFP-RxLR24 signal co-localized with the membrane marker dye FM4-64 (Figure 4b), indicating an association of RxLR24 with the plasma membrane and vesicles with a diameter of approximately 0.8–2 μm (Figure S4). The association of RxLR24 with membranes was confirmed by cellular fractionation performed with leaf tissue of *N. benthamiana* expressing FLAG-RxLR24. RxLR24 was

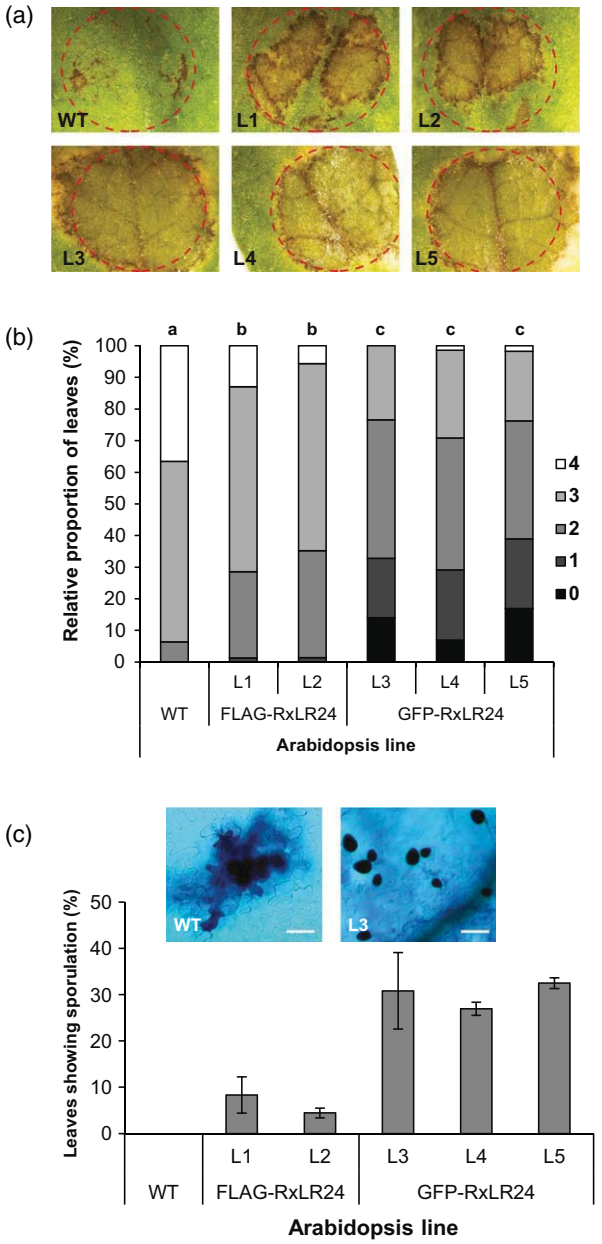

Figure 2. Effect of ectopic RxLR24 expression on disease resistance of Arabidopsis to *Phytophthora brassicae* (CBS 179.87).
Homozygous FLAG-RxLR24 lines (L1 and L2) and hemizygous GFP-RxLR24 lines (L3, L4 and L5) were included in the test.
(a) Disease symptoms 7 dpi of leaves inoculated with a zoospore suspension.
(b) Relative distribution of susceptibility scores based on symptom development measured as lesion size (0 = fully susceptible; 4 = fully resistant). The results are based on two experiments each including 30 fully developed leaves of 10 plants per line. Statistically significant differences labelled with a, b, c based on multiple pairwise comparison using Fisher's exact test ($P < 0.05$; *P*-values adjusted for multiple testing by the method of Benjamini and Hochberg).
(c) Percentage of leaves containing sporangia in wild-type (WT) and RxLR24 lines. The results are derived from two experiments including a total of 60 leaves per line. Insert: zoosporangia formation (dark blue) 7 dpi in the susceptible hemizygous RxLR24 line 3 compared with hypersensitive lesion formation (dark blue) in the resistant WT. Samples were stained with lactophenol-trypan blue. Scale bar: 50 μm. Results represent the mean (± SD) of two experiments.

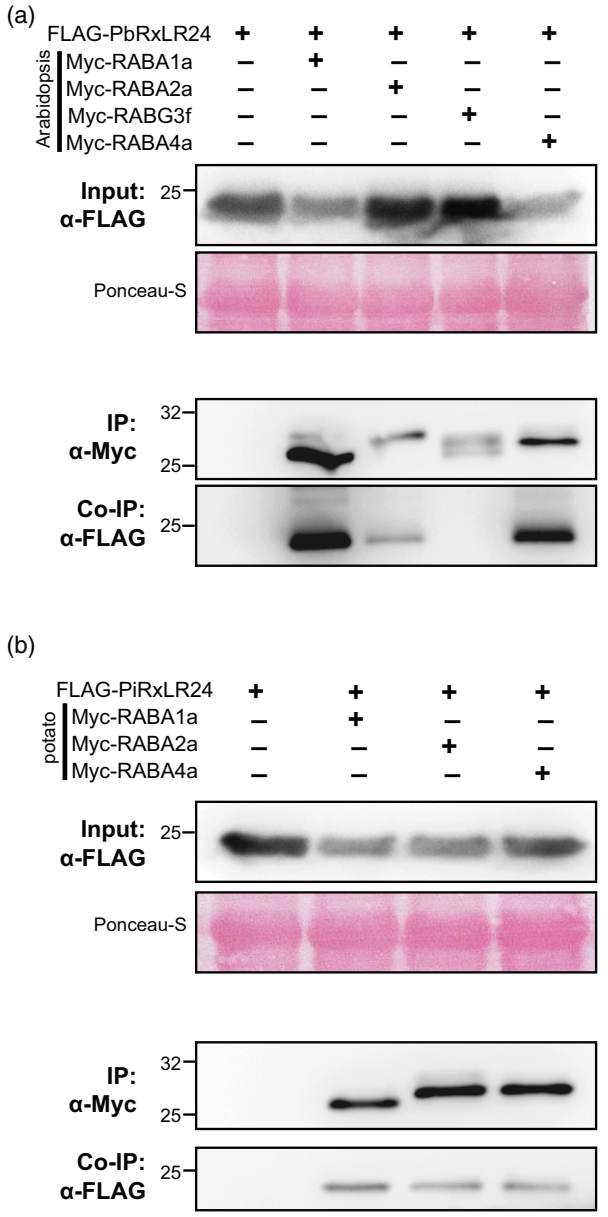

Figure 3. Co-immunoprecipitation (Co-IP) experiments demonstrating interaction between RxLR24 and different RABA GTPases.
Input used for the assays are protein extracts of *Nicotiana benthamiana* leaves infiltrated with combinations of the indicated constructs (+). Control immunoblots show the FLAG-tagged protein input. Ponceau-S (PS)-stained Rubisco large subunit served as a loading control. Immunoprecipitation (IP) of RAB proteins was performed with an anti-Myc antibody (α-Myc). Co-IP of RxLR24 was detected with an anti-FLAG antibody (α-FLAG).
(a) *Pb*RxLR24 of *Phytophthora brassicae* binds to three different RABA family members of Arabidopsis but not to RABG3f.
(b) *Pi*RxLR24 of *Phytophthora infestans* interacts with three different RABA GTPases of potato.

quantitatively associated with the membrane fraction, and this association depended on the presence of the RxLR24 C-terminus as FLAG-RxLR24ΔC accumulated in the soluble fraction (Figure S5). Lack of co-localization with the

membrane dye FM4-64 confirms that GFP-RxLR24ΔC is not associated with membranes (Figure 3c). To compare the subcellular localization of RxLR24 and one of its putative targets, GFP-RxLR24 was co-expressed in *N. benthamiana* together with Arabidopsis RABA1a containing a N-terminal RFP-tag (RFP-RABA1a). The red fluorescence of RFP co-localized with the green fluorescence of GFP in dot-like structures (Figure 4d) and at the cell periphery (Figure 4e). Because RABA proteins are known to localize to vesicles and the plasma membrane (Feraru *et al.*, 2012), we concluded that RxLR24 localizes to vesicles and to the plasma membrane. The results of co-localization analysis were confirmed with intensity profiles taken from pictures shown in Figure 4b–e (Figure S6).

RxLR24 perturbs the secretory pathway

RABA GTPases are involved in vesicle trafficking (Vernoud *et al.*, 2003). Hence, the physical interaction of RxLR24 with members of the RABA subfamily suggested that RxLR24 might interfere with vesicle trafficking. This hypothesis was tested with the help of a fusion construct encoding a secreted pH-sensitive version of GFP (secGFP; Bartetzko *et al.*, 2009), which loses fluorescence upon secretion into the acidic apoplastic space. The secGFP protein was co-expressed with either FLAG-RxLR24, empty vector or FLAG-RxLR24ΔC in leaves of *N. benthamiana*. When co-expressed with an empty vector control, the GFP signal was present in vesicle-like structures (Figure 5a). In the presence of RxLR24 the GFP signal was, however, localized to the reticulate network of the ER and to large round structures. The ER retention of secGFP depended on the presence of the RxLR24 C-terminus as the subcellular distribution of the fluorescence signal in response to co-expression of RxLR24ΔC was similar to the empty vector control. Co-expression with RxLR24 leads to a retention of the GFP signal within cells compared with the two controls, as shown in low-magnification pictures (Figure 5b) and by quantitative analysis of the cellular GFP signal (Figure 5c). The fourfold higher intracellular GFP fluorescence in the presence of RxLR24 was not a result of different levels of GFP expression between the treatments as the total amount of secGFP analysed by immunoblotting were comparable between the experiments (Figure 5d). Together, the results suggest that RxLR24 interferes with protein secretion at the level of the ER.

RxLR24 inhibits the secretion of antimicrobial PR-1 and PDF1.2 proteins

The previous results suggested that RxLR24 may contribute to the virulence of *P. brassicae* via inhibition of secretion of defence-related proteins. To test this hypothesis the effect of RxLR24 on secretion of antimicrobial proteins was analysed. Two cargo proteins were chosen as candidates: PR-1 (PATHOGENESIS-RELATED PROTEIN 1) and DEFENSIN PDF1.2. Transcripts of *PR-1* and *PDF1.2* accumulated in response to inoculation of Arabidopsis leaves with *P. brassicae* (Figure S7), and both proteins are secreted into the extracellular space (Van Loon and Van Strien, 1999; Thomma *et al.*, 2002). To differentiate between cellular and extracellular accumulation, C-terminal fusion constructs were prepared with a pH-sensitive version of GFP (phGFP; Bartetzko *et al.*, 2009) and transiently co-expressed in *N. benthamiana* epidermal cells with either empty vector control or FLAG-RxLR24. Confocal microscopy revealed that RxLR24 affected the subcellular localization of PR-1-phGFP and PDF1.2-phGFP (Figure 6). In control tissue the GFP signal of both proteins was restricted to punctate cellular structures likely to represent secretory vesicles with their respective cargo proteins. Co-expression together with RxLR24, however, led to a dramatic change of the subcellular GFP localization to the reticulate network of the ER and to round bodies of a diameter of about 10 μm. The intracellular retention of PR-1-phGFP and PDF1.2-phGFP in the presence of RxLR24 was also detectable at lower magnification (Figure 7). No GFP-signal derived from phGFP-fusion proteins was detectable in the absence of RxLR24, whereas enhanced GFP fluorescence, indicating cellular retention, was observed in the presence of RxLR24 (Figure 7a). Quantification showed that RxLR24 caused about a three times higher fluorescence emission compared with vector control experiments (Figure 7b), although the total amount of GFP was reduced in the presence of RxLR24 (Figure 7c).

Interestingly, the subcellular localization to vesicles of a third secreted defense-related protein, PLANT NATRIURETIC PEPTIDE A (PNP-A) was not affected by RxLR24 (Figure 6). The total cellular GFP signal was comparable between vector control and RxLR24-expressing plants, suggesting that PNP-A-phGFP was efficiently secreted despite the presence of RxLR24 (Figure 7a and b). Immunoblot analysis revealed similar levels of total PNP-A-phGFP protein in control and RxLR24-expressing *N. benthamiana* leaves (Figure 7c). Another secretion-dependent defence response is callose deposition in the apoplast at sites of pathogen penetration. No difference in local callose accumulation was found between WT Arabidopsis plants and RxLR24 lines in response to inoculation with a zoospore suspension of *P. brassicae* (Figure S8). Our results suggest that RABA-dependent and RABA-independent secretion processes are involved in delivering immunity-related compounds to the apoplast.

DISCUSSION

Considering the shared phylogenetic origin of Phytophthora, it is surprising that only a few of the hundreds of RxLR effectors are highly conserved across species boundaries. For example, comparison of predicted effectors between *Phytophthora sojae*, *Phytophthora ramorum* and

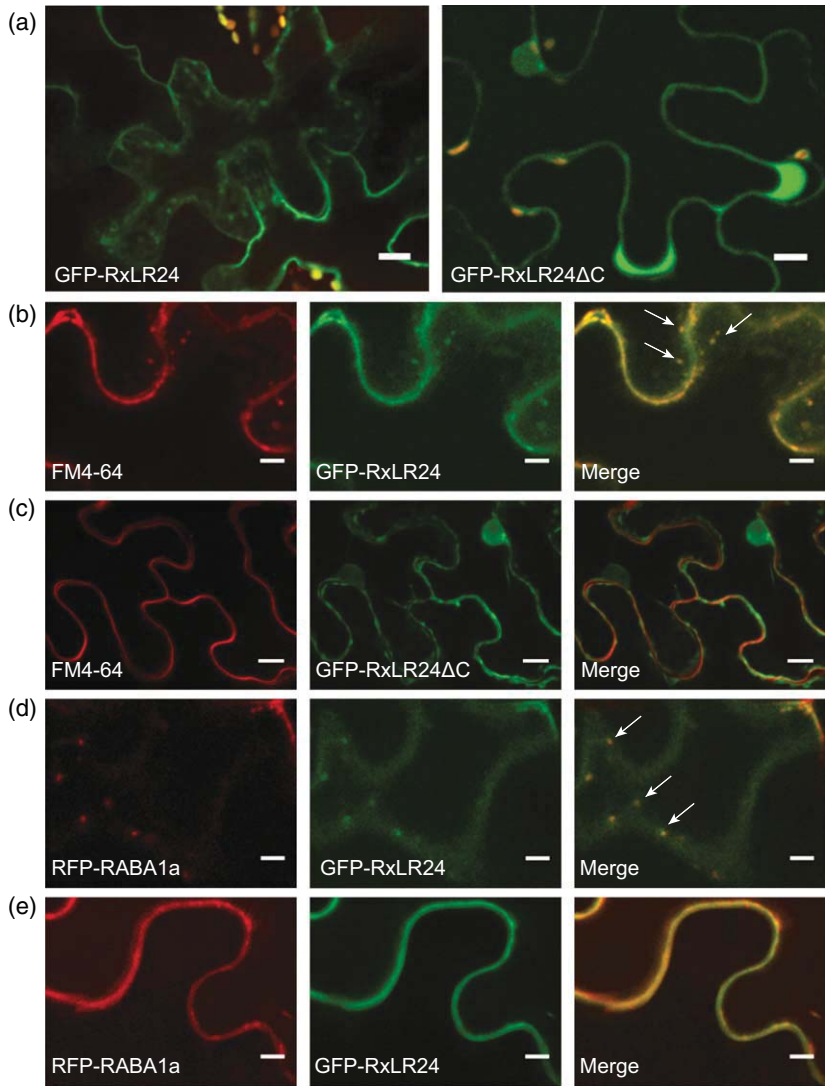

Figure 4. Subcellular localization of *Pb*RxLR24 and selected RABA proteins.
GFP-RxLR24 and RFP-RABA1a were co-expressed in leaves of *Nicotiana benthamiana*.
(a) Left: GFP-RxLR24 localizes to the cell periphery and to dot-like structures in epidermal cells. Right: truncation of the C-terminal effector domain in RxLR24ΔC caused a re-localization of the GFP signal to the cytosol and nucleus. Chloroplast autofluorescence is marked in yellow.
(b) GFP-RxLR24 co-localizes with the FM4-64 dye to plasma membranes and dot-like structures marked with the arrows.
(c) Cytosolic location of RxLR24-ΔC is proven by lack of overlay with membrane dye FM4-64.
(d) Co-localization of GFP-RxLR24 and RFP-RABA1a signals in dot-like structures (arrows).
(e) Co-localization of GFP-RxLR24 and RFP-RABA1a signals at the plasma membrane. Each panel of confocal images shows a single focal plane. Scale bar represents 5 μm (b, d, e) or 10 μm (a and c). For all constructs OD_{600} = 0.1 was used and pictures were taken 24 h after agroinfiltration.

P. infestans identified only 16 effectors that were highly conserved in all three species (Haas *et al.*, 2009). Sequence conservation across species boundaries suggests that such homologous effectors, defined also as core effectors, play important roles in pathogen virulence and share comparable modes of action in different host plants (Anderson *et al.*, 2012, 2015).

Our aim was to functionally characterize the conserved effector *Pb*RxLR24 of the Arabidopsis pathogen *P. brassicae* and its homologue *Pi*RxLR24 of *P. infestans*. As observed with other effectors (Haas *et al.*, 2009; Wang *et al.*, 2011a; Anderson *et al.*, 2012), *PbRxLR24* transcript level was induced upon contact of *P. brassicae* with the host, and constitutive expression of *Pb*RxLR24 directly in Arabidopsis resulted in enhanced disease symptoms and positively influenced asexual reproduction of *P. brassicae*. Hence, *Pb*RxLR24 has an immunity-relevant host target in Arabidopsis. This target is also required for processes beyond immunity as Arabidopsis plants expressing high levels of *Pb*RxLR24 were dwarfed. The correlation between

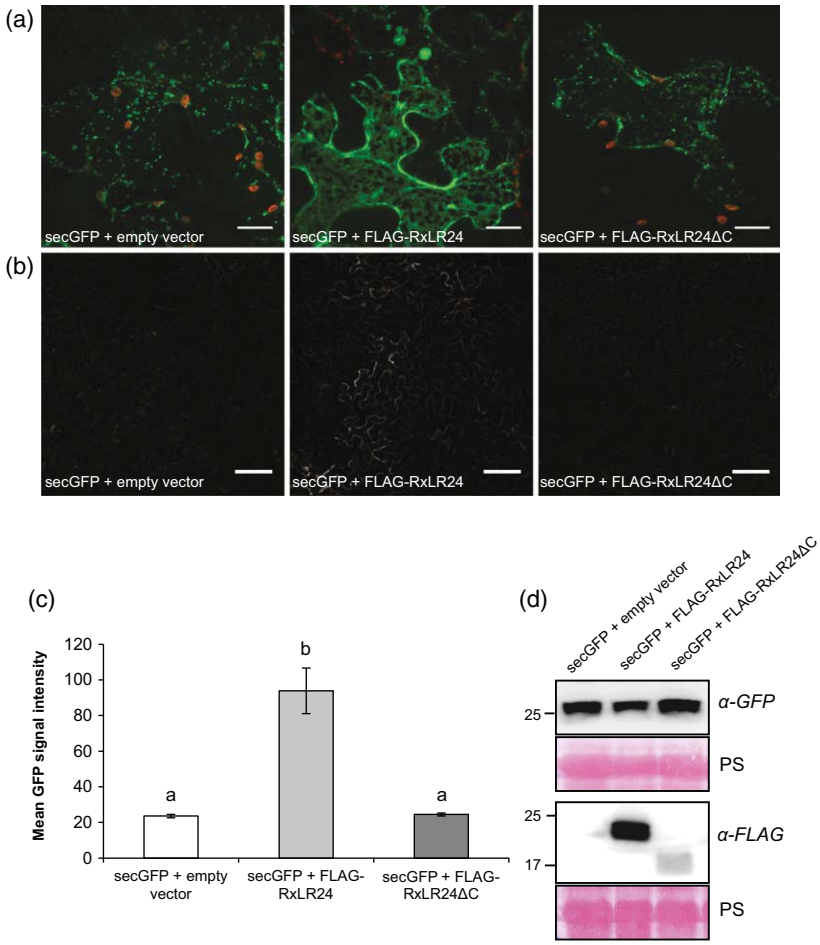

Figure 5. Effect of RxLR24 on the secretion of pH-sensitive GFP (phGFP).
Leaves of *Nicotiana benthamiana* were agroinfiltrated with a fusion construct encoding a secreted version of phGFP (secGFP), which loses fluorescence in the acidic extracellular space. OD_{600} for agroinfiltration was 0.1 for secGFP and 0.3 for effector and empty vector constructs. Samples were analysed by confocal microscopy 48 h after agroinfiltration.
(a) GFP fluorescence is present in dot-like structures in the absence of RxLR24 (empty vector) and in the presence of RxLR24ΔC, respectively. In the presence of RxLR24 the GFP signal is retained in the reticulate network of the endoplasmic reticulum (ER) and large round structures. Each photo represents a stack of 15 images. Chloroplast autofluorescence is marked in red. Scale bar: 20 μm.
(b) No GFP signal is visible at a six times lower magnification compared with (a) in the absence of RxLR24 (empty vector) or in the presence of RxLR24ΔC. Co-expression of RxLR24 traps fluorescent secGFP in the symplast. Photos after background subtraction. Scale bar: 100 μm.
(c) Quantification of fluorescence representing symplasmic GFP. Quantification for each construct combination was performed on 48 confocal images collected from three plants. Two leaves per plant were analysed at eight randomly chosen locations. The eight results obtained per leaf were pooled together as one mean value. Results represent the mean (± SD) obtained for six leaves. Statistically significant differences between group means were determined by one-way ANOVA at the $P < 0.05$ level for $F_2 = 176.5$, $P = 3.77E\text{-}11$ and labelled with a and b based on Tukey (HSD) multiple comparisons of means ($P < 0.05$). The experiment was repeated once with similar results.
(d) Verification of expression of FLAG-RxLR24 and secGFP by immunoblot analysis with anti-FLAG or anti-GFP antibodies, respectively. Ponceau-S (PS)-stained Rubisco large subunit served as a loading control.

expression level and growth phenotype indicated that increasing *Pb*RxLR24 levels titre a function that is important for plant development. Plant immunity was, however, more sensitive to *Pb*RxLR24 than plant growth as transgenic lines with a WT growth phenotype were compromised in their disease resistance towards *P. brassicae*. RxLR24 expression had no significant impact on disease resistance towards the fungal pathogen *B. cinerea*. Because multiple components contribute to disease resistance, it is not possible to draw conclusions from this negative result with regard of the importance of secretion for resistance towards *B. cinerea*.

Our conclusion that *Pb*RxLR24 proteins physically interact with members of the RABA GTPase family is supported by several lines of evidence. First, untargeted immunoprecipitation of FLAG-*Pb*RxLR24 expressed in Arabidopsis followed by mass spectrometry identified as the 11 top hits different RABA GTPases belonging to the subfamilies RABA1, RABA2 and RABA4. In contrast, negative control experiments with FLAG-tagged versions of three unrelated

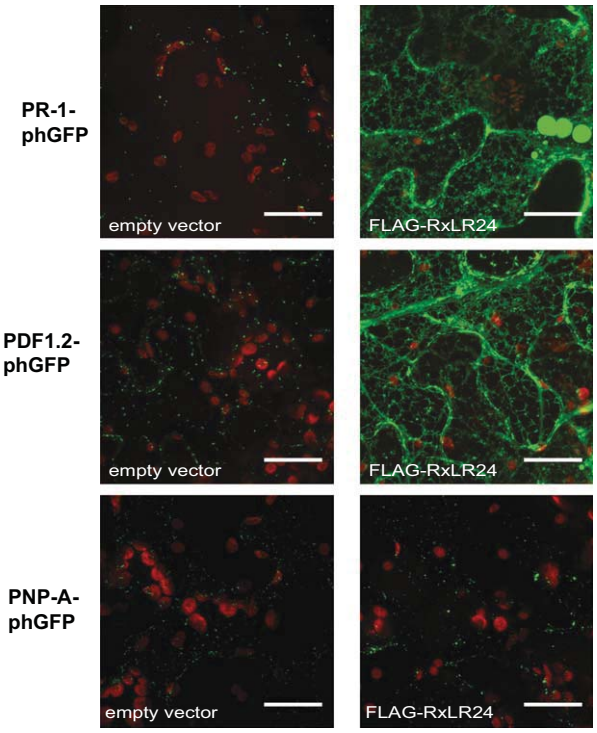

Figure 6. Effect of RxLR24 on secretion of host defence proteins.
The effect of RxLR24 on the localization of phGFP-tagged defence proteins was analysed in agro-infiltrated *Nicotiana benthamiana* leaves. OD_{600} for agroinfiltration was 0.1 for phGFP-tagged protein vectors, and 0.3 for effector and empty vector constructs. Pictures were taken 48 h after agroinfiltration. Left panel: co-expression of PR-1-phGFP, PDF1.2-phGFP and PNP-A-phGFP together with empty vector control. Right panel: co-expression of phGFP fusion proteins together with FLAG-RxLR24. Scale bar: 25 μm. Chloroplast autofluorescence marked in red. Each confocal microscopy picture represents a stack of 37–73 single slices.

P. brassicae RxLR effectors did not give a single hit for a RABA-derived peptide. Second, the physical interaction of RxLR24 with three RABA GTPases, RABA1a, RABA2a and RABA4a, was confirmed by targeted reciprocal immunoprecipitation experiments with agro-infiltrated *N. benthamiana* co-expressing Myc-tagged RABA versions and FLAG-*Pb*RxLR24. Similarly, also *Pi*RxLR24 of *P. infestans* was co-immunoprecipitated with each of three Myc-tagged RABA GTPases of potato. Hence, the homologues of *P. brassicae* and *P. infestans* both interacted with members of the RABA GTPase family. Third, *Pb*RxLR24 and Arabidopsis RABA1a co-localized to the plasma membrane and to vesicles. Fourth, in line with a function of RABA GTPases in vesicle-mediated secretion the ectopic expression of *Pb*RxLR24 inhibited the secretory process leading to an accumulation of secretory proteins in the ER. Together these results provide evidence that RxLR24 effectors target members of the RABA GTPases subfamily to inhibit vesicular secretion.

In the classical secretory pathway, newly synthesized proteins are transported from the ER to the Golgi via vesicles, and from there to the trans-Golgi network (TGN) to be delivered to either the plasma membrane or as cargo by exocytosis to the extracellular space. The secretory pathway depends on the activity of small GTPases that cycle between an active GTP-bound membrane-associated state and an inactive GDP-bound cytosolic state. Activation is catalysed by specific guanine nucleotide exchange factors (GEFs), and inactivation is mediated by GTPase-activating proteins (GAPs; Vernoud *et al.*, 2003; Stenmark, 2009). Small GTPases are divided into three families: RAB GTPases; ROP GTPases (Rho of plants); and ARF GTPases (ADP-ribosylation factor). RAB GTPases form the largest group of small GTPases in plants (Stenmark, 2009). The Arabidopsis genome encodes 57 members that are grouped into eight clades (RABA-RABH; Vernoud *et al.*, 2003). Interestingly, RABA forms the largest subclade consisting of 26 members. The extension of the RABA GTPase family in plants compared with the corresponding RAB11 family in mammals (three members) and Ypt31/32 in yeast (two members) suggests plant-specific functions of some RABA proteins. Together with their regulatory proteins, RABA GTPases play a role in anterograde vesicle transport from the TGN to the plasma membrane, and they may also function in endocytosis (Chow *et al.*, 2008; Feraru *et al.*, 2012).

The analysis of subcellular localization and the results from membrane fractionation experiments revealed that *Pb*RxLR24 associates with membranes. Membrane anchoring of RAB GTPases is mediated by geranylgeranylation of cysteine residues at the C-terminus (Hutagalung and Novick, 2011). RxLR24 proteins contain neither an integral membrane domain nor any prenylation or myristoylation sites. The subcellular localization to plasma and vesicular membranes is most likely the result of binding of *Pb*RxLR24 to membrane-localized RABA proteins. This hypothesis is difficult to test as it would require combined knockout of all interacting RABA GTPases that is expected to be lethal considering the dwarfed phenotype of Arabidopsis plants with partially inhibited RABA protein functionality. It is clear that the RABA binding domain resides in the C-terminal part of *Pb*RxLR24. Deletion of the C-term in RxLR24ΔC abolished binding to RABA proteins and caused redirection of the truncated effector to the cytoplasm. The loss of RABA and membrane association of RxLR24ΔC correlated with a loss of the ability to inhibit secretion of secGFP. Many RABA family members were previously shown to localize to vesicles transporting cargo from the TGN to the plasma membrane (Qi and Zheng, 2013; Berson *et al.*, 2014), and localization to the plasma membrane was reported for RABA1b (Feraru *et al.*, 2012) and RABA4c (Ellinger *et al.*, 2014) both of which are included in our list of RxLR24 interacting proteins. Hence, the co-localization of *Pb*RxLR24 and RABA proteins indicates that RxLR24 associates with the TGN and with the plasma membrane.

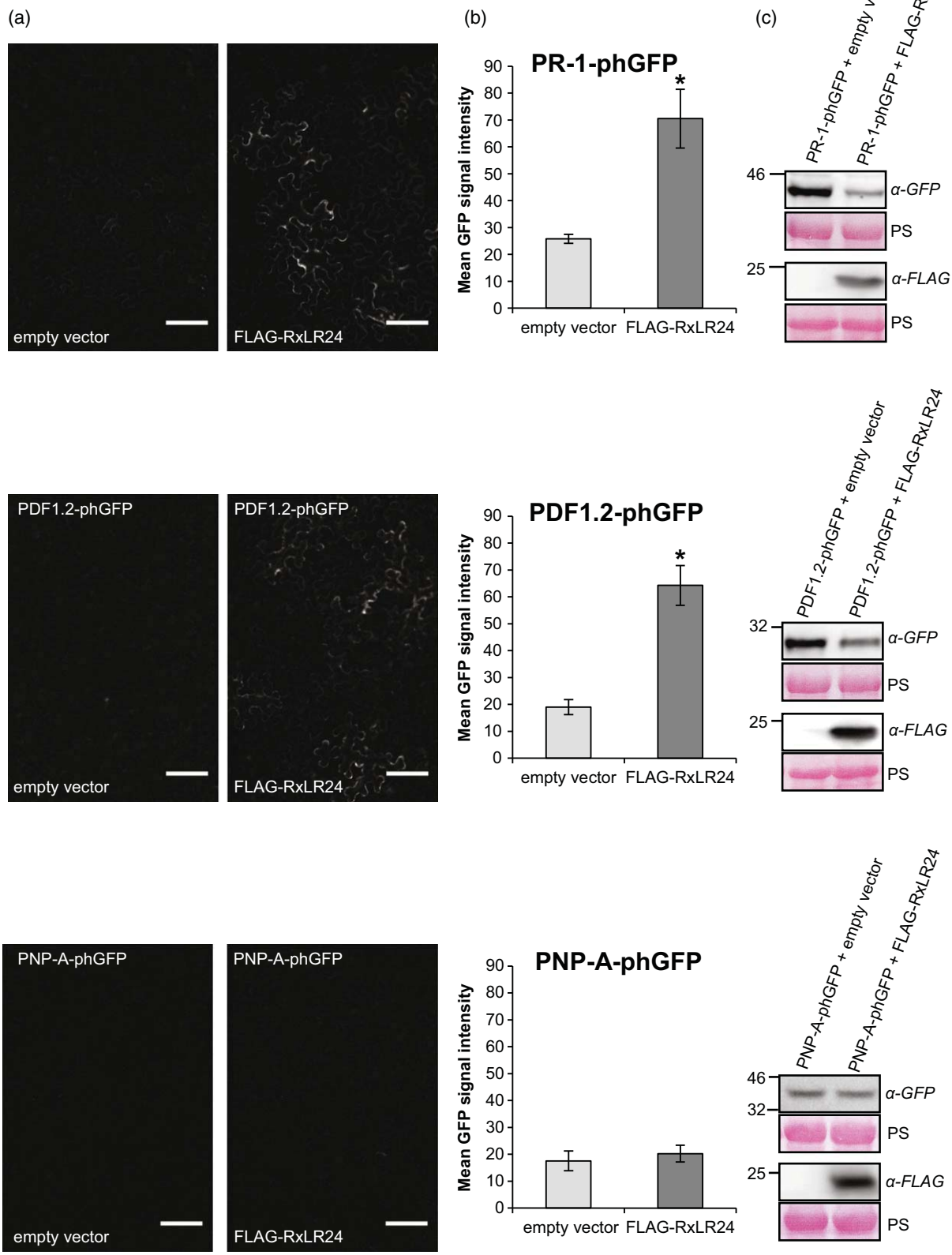

Figure 7. Effect of RxLR24 on secretion of host defence proteins.
PR-1-phGFP, PDF1.2-phGFP and PNP-A-phGFP were individually expressed in leaves of *Nicotiana benthamiana* together with either empty vector control or FLAG-RxLR24. OD_{600} for agroinfiltration was 0.1 for phGFP-tagged protein vectors, and 0.3 for effector and empty vector constructs. Pictures were taken 48 h after agroinfiltration.
(a) Confocal microscopy of GFP signal in epidermal cells expressing the indicated phGFP-fusion proteins in the presence or absence of FLAG-RxLR24. Each picture shows a representative area of 500 × 730 μm. Background subtraction was applied to make the pictures comparable. Scale bar: 100 μm.
(b) Quantification of GFP fluorescence of the experiments shown in (a). Quantification for each construct combination was performed on 48 confocal images collected from three plants. Two leaves per plant were analysed at eight randomly chosen locations. These eight results obtained for each leaf were pooled together as one mean value. Results represent the mean (± SD) obtained for six leaves in single experiment. Statistically significant differences between group means were determined by Student's *t*-test and labelled with an asterisk ($P < 0.05$). The experiment was repeated once with similar results.
(c) Immunoblot showing that all constructs were correctly expressed. Ponceau-S (PS)-stained Rubisco large subunit served as a loading control.

Functional analysis of RABA GTPases is mainly based on Arabidopsis knockout mutants. Single knockout mutants of RABA1a, RABA1b, RABA1c and RABA1d exhibited normal growth phenotypes, and the quadruple mutant only had slightly shorter roots than WT plants (Asaoka *et al.*, 2013). Similarly, no effect on growth was observed for single Arabidopsis knockout mutants, such as *raba1a*, *raba1c*, *raba1d*, *raba1i*, *raba2b*, *raba2d*, *raba3*, *raba4a*, *raba4b* and *raba4e* (Lunn *et al.*, 2013). The lack of developmental phenotypes is most likely caused by functional redundancy within the large RABA family. In contrast to single or multiple RABA mutants, expression of *Pb*RxLR24 leads to a dose-dependent reduction of plant growth. The fact that RxLR24 had a stronger effect on plant development than multiple knockouts of RABA family members supports the conclusion that RxLR24 interacts with many RABA GTPases. The initial screen for RxLR24 interacting partners identified 11 RABA proteins as top candidates. Considering that some RABA proteins are only weakly or not expressed in leaves (Szumlanski and Nielsen, 2009), it seems likely that *Pb*RxLR24 interacts with the majority of RABA proteins. We provide no experimental evidence about how exactly RxLR24 might interfere with RABA functionality. In principle, RxLR24 binding could interfere with RABA regulation, with the association to the cytoskeleton or with the binding to specific proteins located in target membranes. As *Pb*RxLR24-positive vesicles remained mobile, attachment to the cytoskeleton seems to be functional.

The role of RABA proteins has been mainly addressed in the context of plant development. RABA1d (Berson *et al.*, 2014) as well as members of RABA2 and RABA3 subclasses were shown to be involved in cell plate formation (Chow *et al.*, 2008), and lack of RABA4d caused abnormal shape of pollen tubes with altered localization of pectin (Szumlanski and Nielsen, 2009), and some RABA GTPases have been reported to play a role in cell wall formation (Lunn *et al.*, 2013). Little is known, however, about the role of RABA proteins in abiotic or biotic stress. Members of the RABA1 clade were required for salinity stress tolerance, but their precise role remained unclear (Asaoka *et al.*, 2013). RABA4c over-expression in Arabidopsis led to penetration resistance against the powdery mildew pathogen *Golovinomyces cichoracearum* (Ellinger *et al.*, 2014). Interestingly, RAB11 of *Drosophila melanogaster* (homologous to plant RABA GTPases) was shown to play a role in the vesicular delivery of the antimicrobial peptide drosomycin to the haemolymph, and inhibition of drosomycin secretion resulted in higher death rates after infection with bacteria (Shandala *et al.*, 2011).

The physical interaction of RxLR24 with RABA GTPases is expected to affect the secretory process. We used a secreted pH-sensitive version of GFP (secGFP; Bartetzko *et al.*, 2009) to test this hypothesis. Because secretion to the acidic intercellular space causes loss of GFP fluorescence, secGFP functions as a tool to distinguish between cellular and extracellular GFP accumulation (Zheng *et al.*, 2005; Bartetzko *et al.*, 2009). Co-expression of *Pb*RxLR24 and secGFP in *N. benthamiana* leaves caused cellular retention of GFP-fluorescence that was not observed in vector control plants. This effect was not an artefact of unequal GFP production. The results show that *Pb*RxLR24 interferes with the secretion of secGFP, and caused its retention in the ER and in large round structures. We can only speculate about the causes of secGFP retention in ER. The most straightforward explanation is that RxLR24 inhibits the activity of RABA proteins associated with vesicle budding at the ER. This would, however, be unusual as RABA GTPases are described as markers of TGN (Vernoud *et al.*, 2003; Qi and Zheng, 2013; Berson *et al.*, 2014), and association with ER was considered as a side-effect of over-expression (Rehman *et al.*, 2008). We have tested the subcellular localization of RABA1a and did not find indications of ER localization. An alternative explanation for ER retention of secretory proteins would be that *Pb*RxLR24 negatively affects the regulation of RABA GTPases in the TGN resulting in a traffic jam that feeds back to the ER. Consistent with this interpretation, a non-functional mutant version of tomato RABA1a with an inactive GTP binding site caused a partial retention of secGFP in the ER (Rehman *et al.*, 2008).

The secretory process has been shown to be targeted by a number of pathogen effectors. The most prominent example is the macrocyclic lactone brefeldin A that has become an important tool for studying secretory processes. The bacterial pathogen *P. syringae* produces the

type III effector HopM1 that physically binds to the Arabidopsis protein AtMIN7 to initiate its degradation (Nomura *et al.*, 2006, 2011). AtMIN7 encodes an ARF-GEF, which is an activator of ARF GTPases localized in TGN and involved in vesicle trafficking. Two other bacterial type III effectors were shown to inhibit protein secretion, although their host target remained unknown (Bartetzko *et al.*, 2009; Schulze *et al.*, 2012). The powdery mildew effector BEC4 targets an ARF-GAP involved in the activation of ARFs and contributes to enhanced virulence (Schmidt *et al.*, 2014). The RxLR effector Avr1 of *P. infestans* interacts with the exocyst component Sec5 and affects secretion of PR-1 and callose deposition (Du *et al.*, 2015). Another RxLR effector of *P. infestans*, AVRblb2, was shown to interfere with the secretion of a plant immune protease (Bozkurt *et al.*, 2011).

Many plant immune responses depend on functional secretion of vesicle cargo and on the delivery of membrane proteins to the cell surface. The classical example is secretion of antimicrobial proteins, such as PR-1 and PDF1.2, into the apoplast to inhibit the early colonialization of the intercellular space. Co-expression of *Pb*RxLR24 together with phGFP-tagged PR-1 or PDF1.2 in *N. benthamiana* resulted in their intracellular retention. Similar to the results with secGFP, PR-1 and PDF1.2 accumulated in the ER. The secretion of PR-1 and PDF1.2 appears to depend on RABA-positive vesicles, and *Pb*RxLR24 likely contributes to host plant susceptibility via restriction of PR-1 and PDF1.2 secretion. Because the defence functions of many immunity-related compounds depend on a functional secretory pathway, it is not possible to quantify the contribution of reduced secretion of the two antimicrobial proteins to the enhanced disease susceptibility phenotype of *Pb*RxLR24-expressing Arabidopsis lines.

Surprisingly, the secretion of the stress-induced protein PNP-A, whose role in abiotic and biotic defence is not yet clear (Wang *et al.*, 2011b), was not affected by *Pb*RxLR24. Apparently, stress-associated proteins are secreted by both RABA-dependent and RABA-independent pathways. Similarly, the accumulation of local callose depositions in response to *P. brassicae* was not affected by *Pb*RxLR24 in Arabidopsis, suggesting functional delivery of the ß-1,3-glucan synthase PMR4 and its substrates by RABA-independent pathways. It remains to be seen whether or not *Pb*RxLR24 affects transport and targeting of other immune relevant compounds.

In summary, RxLR24 effectors of *P. brassicae* and *P. infestans* interact with members of the RABA GTPase subfamily that play roles in the transport of vesicles from the TGN to the plasma membrane. The interaction causes an inhibition of secretory processes that export the antimicrobial proteins PR-1, PDF1.2 and possibly other defence-related compounds, which may explain the observed enhanced disease susceptibility of *Pb*RxLR24 expressing Arabidopsis lines towards *P. brassicae*. With regard to functional diversification in plants, our results provide evidence for a specific function of RABA GTPases in the secretory process that cannot be fully substituted by other subclades of the RAB GTPase family. Because the RxLR24 effector targets many RABA GTPases, it can be used in the future as a molecular tool to better define RABA GTPase-mediated vesicular transport.

EXPERIMENTAL PROCEDURES

Identification of RxLR24 homologues

RxLR effector candidates identified in an EST library of *P. brassicae* were used for a blast similarity search for corresponding RxLR effector homologues of other Phytophthora species (NCBI database Phytophthora taxid: 4783). One of the identified conserved effector candidates, named *Pb*RxLR24, was chosen for further analysis. The amino acid sequence of *Pb*RxLR24 was used for sequence alignment with homologues from selected Phytophthora species using Clustal Omega (https://www.ebi.ac.uk/Tools/msa/clustalo/) and BoxShade (https://embnet.vital-it.ch/software/BOX_form.html). Signal peptides identified with SignalP 4.1 (http://www.cbs.dtu.dk/services/SignalP/) were excluded from sequence comparisons.

Biological material and disease resistance tests

Nicotiana benthamiana plants were grown under 16 h light at 28°C and 8 h of darkness at 25°C. Arabidopsis plants accession Wassilewskija (Ws-0) were cultivated with a 12 h light cycle, and 21°C daytime temperature and 19°C night temperature. For tests of disease resistance, the adaxial leaf surface of 3-week-old Arabidopsis plants was inoculated with 30 µl droplets of a zoospore suspension (10^5 zoospores ml^{-1}) of the *P. brassicae* isolate CBS 179.87 (Roetschi *et al.*, 2001). Three fully developed leaves per plant were inoculated, and 10 plants per genotype were used in each test. The Arabidopsis double mutant *cyp79B2 cyp79B3* was used as a susceptibility control, and disease resistance was evaluated based on lesion size according to a previously described scale (Schlaeppi *et al.*, 2010). Inoculation with *B. cinerea* strain BMM was performed as described (L'Haridon *et al.*, 2011). Four leaves per plant were infected with a 6 µl droplet of a spore suspension (2×10^5 spores ml^{-1}). Lesion size was measured 3 days after infection. Two independent experiments were performed with similar results. In total, 32 plants per genotype were tested.

Cloning and bacterial transformation

Gene-specific primers, cDNAs, destination vectors and final fusion proteins are listed in Table S3. PCR amplifications were performed using Phusion® High-Fidelity DNA Polymerase (New England Biolabs). The amplification products were cloned into pENTR (pENTR™/D-TOPO® Cloning Kit; Invitrogen) and transformed into *Escherichia coli* XL1 Blue cells. Following sequence verification, the cDNA inserts were mobilized into Gateway destination vectors to be used for transformation of *Agrobacterium tumefaciens* strain GV3101 by the freeze–thaw method. The construction of fusion proteins containing phGFP was based on a pENTR1a plasmid containing the cDNA of phGFP (Bartetzko *et al.*, 2009) with deleted signal peptide sequence. After sequence verification and restriction digestion, the PCR product was cloned into pENTR1a using *Xho*I and *EcoR*V restriction sites to create pENTR1a:phGFPΔSP. PR-1, PDF1.2 and PNP-A cDNAs were cloned into *Not*I and *Sal*I restriction sites of pENTR1a:phGFPΔSP. The C-terminal sequence

of RxLR24 starting with amino acid position 105 was removed by PCR to create the truncated FLAG-RxLR24ΔC fusion protein.

Agroinfiltration of *Nicotiana benthamiana*

Agrobacterium tumefaciens strain GV3101 was used for agroinfiltration experiments as described (Schütze *et al.*, 2009). Leaves of 3–4-week-old *N. benthamiana* plants were infiltrated with a 1:1 mixture of Agrobacterium containing the respective construct and a P19 silencing suppressor strain. The concentration of Agrobacterium suspensions used for agroinfiltration was adjusted depending on the experiment. A suspension with an OD_{600} of 0.1 was used for localization experiments. To visualize secretion of phGFP, a suspension with an OD_{600} of 0.1 was used for secGFP, PR1-phGFP, PDF1.2-phGFP and PNP-A-phGFP, whereas the OD_{600} of the bacterial suspension for agroinfiltration of FLAG-RXLR24, empty vector control and P19 was adjusted to 0.3. For all other assays the bacterial suspensions were adjusted to an OD_{600} of 0.7. The agroinfiltrated plants were incubated for 24 h for localization experiments, 48 h for the observation of secGFP and phGFP-tagged protein secretion, and 72 h for all other experiments.

Arabidopsis transformation

Arabidopsis thaliana accession Ws-0 was transformed by the floral dip method (Clough and Bent, 1998). Transformed plants were selected either depending on red fluorescence emission in the seeds (for GFP-RxLR24 plants; Shimada *et al.*, 2010) or by screening with BASTA (for FLAG-RxLR24 plants). Transformants were tested for transgene expression by qPCR analysis and immunoblotting following standard procedures. Homozygous FLAG-RxLR24 over-expressing lines carrying one copy of the transgene were selected based on segregation analysis.

Membrane fractionation

Microsomal membrane fractions were isolated from 200 mg of *N. benthamiana* leaf tissue expressing FLAG-RxLR24 or FLAG-RxLR24ΔC. Preparation of the microsomal fraction was performed as previously described (Abas and Luschnig, 2010). Soluble proteins were precipitated with TCA and washed with cold acetone. The precipitated soluble proteins and the pellet of the microsomal fraction were solubilized in 30 μl sodium dodecyl sulphate (SDS) sample buffer, and the total fractions were subjected to SDS–polyacrylamide gel electrophoresis (PAGE) analysis.

Immunoprecipitation and MS analysis

Immmunoprecipitation experiments were based on FLAG-tagged RxLR24 constructs and included as negative controls FLAG-tagged version of three unrelated RxLR effectors of *P. brassicae* (Table S2). Leaves of 5-week-old Arabidopsis plants expressing tagged effector proteins were frozen in liquid nitrogen and ground to a fine powder. Proteins were extracted from 6 g of plant tissue using ice-cold extraction buffer (25 mM HEPES, pH 7.4, 150 mM NaCl, 0.5% TritonX-100, 1 mM EDTA) supplemented with Sigma FAST™ Protease Inhibitor tablets (1 tablet per 50 ml extraction buffer). All steps were performed at 4°C. After 1 h of incubation on a stirring wheel, samples were centrifuged for 15 min at 15 000 ***g*** and filtered with PES syringae filters of 0.22 μm. Protein concentrations of supernatants were adjusted to 1 mg ml^{-1} using the Bradford protein assay. The samples were incubated for 4 h with 50 μl packed volume of capture resin (ANTI-FLAG M2 Magnetic Beads, Sigma). Beads were collected by a magnet and subsequently washed as recommended by the manufacturer. The collected beads were used to identify proteins co-purifying with FLAG-RxLR24 by LC-MS/MS performed by the Protein Analysis Facility (Center for Integrative Genomics, Faculty of Biology and Medicine, University of Lausanne, Switzerland). MS data search was performed with engine Mascot Version 2.4.1. Identified peptides were matched to protein sequences with use of the Swiss-Prot_ID 2013_12 & Trembl_ID 2013_1 databases containing 54 189 *A. thaliana* proteins as well as sequences of common contaminants. Results of Mascot search were processed with Scaffold_4.3.3 software. Experiment-wide grouping with protein cluster analysis was applied to group proteins. Peptide threshold was set as 90% minimum. Only proteins identified with confidence match minimum of 95% and at least two unique peptides were considered as reliable result. To verify effector-target interaction FLAG-tagged construct of RxLR24 from *P. brassicae* and its homologue from *P. infestans* were transiently expressed alone in *N. benthamiana* (as negative control) and in combination with selected Myc-tagged RAB proteins from Arabidopsis and potato, respectively. Half a gram of tissue was used for the reciprocal Co-IP experiment employing mouse monoclonal Myc antibody (9E10: sc-40; Santa Cruz Biotechnology) and agarose beads (sc-2003; Santa Cruz Biotechnology) to immunoprecipitate Myc-Rab proteins. Forty microlitres of antibody and 80 μl of beads were used for each sample. The samples were processed as described above. After the final washing step, the proteins collected on agarose beads were solubilized in 50 μl of SDS sample buffer, and 25-μl aliquots were analysed by SDS–PAGE and immunoblotting.

Staining procedures

Lactophenol-trypan blue staining of pathogen structures was performed as published before (Koch and Slusarenko, 1990). Staining for callose (Ton and Mauch-Mani, 2004) was performed on 15 plants per treatment using three leaves per plant. The experiment was repeated once with similar results. Staining with the plasma membrane marker dye FM4-64 was performed by syringe infiltration of a 20 μM dye solution through the abaxial surface of leaves (Rigal *et al.*, 2015).

RNA extraction, cDNA synthesis and qPCR

Total RNA was extracted with the Spectrum Plant Total RNA Kit (Sigma). Two micrograms of total RNA was used for cDNA synthesis (Omniscript Reverse Transcription Kit; Qiagen). The mix for qPCR reactions contained 7.5 μl of SYBR Green (Bioline), cDNA (corresponding to 100 ng RNA) and primers at a concentration of 10 μM in a final volume of 15 μl. Runs were performed on a MIC qPCR machine (Bio Molecular Systems). The final PCR products were analysed by melting point analysis. The transcript level of *RxLR24* effector expressed during infection was determined with *P. brassicae* isolate CBS 179.87 growing on susceptible *cyp79B2 cyp79B3* Arabidopsis plants (Schlaeppi *et al.*, 2010). Leaf discs of 6 mm diameter were cut around inoculation sites. Twelve leaf discs from six plants were analysed per time point. The relative transcript level of *RxLR24* in *P. brassicae* was determined with *ß-tubulin* and *actin* of *P. brassicae* as reference genes. Calculation of the relative expression values was done as described (Vandesompele *et al.*, 2002). Transcript levels of *PR-1*, *PDF1.2* and *PNP-A* in Arabidopsis plants were calculated with *expG* as reference gene (Czechowski *et al.*, 2005) and the comparative cycle threshold method (ΔΔCt). Each experiment was performed at least twice with similar results. qPCR primers used in this study are listed in Table S4.

Protein analysis

Sodium dodecyl sulphate–PAGE and immunoblotting were performed with standard procedures. FLAG-tagged proteins were

detected with monoclonal ANTI-FLAG®M2-Peroxidase (Sigma). Detection of the Myc-tag was based on Myc antibody conjugated with horseradish peroxidase (HRP; Santa Cruz Biotechnology) and anti-GFP antibody conjugated with HRP (Santa Cruz Biotechnology) were used for detection of GFP.

Confocal microscopy

Confocal microscopy was performed with a VisiScope CSU-W1 Spinning Disk Confocal Microscope equipped with Evolve 512 (Photometrics) EM-CDD camera and Scientific Grade 4.2 sCMOS camera. The following excitation wavelengths were used: 488 nm (200 MW) for GFP; and 515 nm (100 MW) for RFP. The emission collected for GFP was done with a BP filter (525/50 nm), and for RFP with a LP filter (575 nm). Images were projected and processed with use of ImageJ software (https://imagej.net). All stacks (voxel depth was 0.8 μm) were prepared with max intensity projection type. Figure preparation is based on Adobe Photoshop and Adobe Illustrator.

Analysis of phGFP accumulation

SecGFP- and phGFP-tagged proteins were transiently co-expressed with empty vector control or FLAG-RxLR24 in *N. benthamiana*. Transformed tissue was imaged by confocal microscopy with a low magnification lens (× 10) and sCMOS camera. Quantification for each construct combination was based on 48 pictures obtained from three plants (2 leaves per plant, 8 pictures per leaf). The size of a single picture taken for measurement was 1331 × 1331 μm. Mean values of signal intensity were calculated as described before (Zavaliev and Epel, 2015). The experiment for each investigated cargo protein was performed at least twice with similar results.

ACCESSION NUMBERS

*Pb*RxLR24 (MG489826), *Pi*RxLR24 (XP002997548/PITG 18405), *P. parasitica* RxLR24 (XP008915662), *P. sojae* RxLR24 (XP009516297), *P. nicotianae* RxLR24 (KUF87794), *Pb*RxLR23 (MG489827), *Pb*RxLR27 (MG489828), *Pb*RxLR29 (MG489829), *P. brassicae* actin (ES289919), *P. brassicae* β-tubulin (ES283175), PR-1 (AT2G14610), PDF1.2 (AT5G44420), PNP-A (AT2G18660), ExpG AT4G26410), *Arabidopsis thaliana* RABA1a (AT1G06400), *Arabidopsis thaliana* RABA2a (AT1G09630), *Arabidopsis thaliana* RABA4a (AT5G65270), *Solanum tuberosum* RABA1a (XM_006348832), *Solanum tuberosum* RABA2a (XM_006349248), *Solanum tuberosum* RABA4a (XM_006353154).

ACKNOWLEDGEMENTS

The authors are thankful to Boris Egger, Stéphanie Kaeser-Pebernard and members of Anna Jazwinska Lab from University of Fribourg, Switzerland, for technical help and sharing facilities. The secGFP construct was a kind gift of Frederik Börnke, Leibniz-Institute for Vegetable and Ornamental Crops (IGZ), University of Potsdam, Germany. The authors also would like to acknowledge Karin Schumacher (Heidelberg University, Germany), as well as Silke Robatzek and Sophien Kamoun (The Sainsbury Laboratory, UK) for helpful discussions. Finally, the authors thank Jadwiga Śliwka (Plant Breeding and Acclimatization Institute-National Research Institute, Poland) for her collaboration during the initial phase of the project. The project was supported by grants of the Swiss National Science Foundation (31003A 129696) and by Sciex (NMS^{ch} 12.283).

CONFLICT OF INTEREST

The authors declare no conflict of interest.

SUPPORTING INFORMATION

Additional Supporting Information may be found in the online version of this article.

Figure S1. Amino acid sequence alignment of RxLR24 effector homologs. Identical amino acids are highlighted in black and similar residues are shown as grey boxes. Sequences encoding signal peptides (SP) are not included. RxLR and dEER motifs are marked with asterisks. Sequence accessions: *P. brassicae* RxLR24 (MG489826), *P. infestans* RxLR24 (XP002997548/ PITG 18405), *P. parasitica* RxLR24 (XP008915662), *P. sojae* RxLR24 (XP009516297) and *P. nicotianae* RxLR24 (KUF87794).

Figure S2. Relative RxLR24 expression of *P. brassicae* during infection of Arabidopsis. Leaves of the susceptible Arabidopsis mutant *cyp79B2_cyp79B3* were drop-inoculated with a zoospore suspension and *PbRxLR24* transcript levels were determined by qPCR. *β-tubulin* and *actin* of *P. brassicae* served as reference transcripts. The relative expression of RxLR24 at 96 hpi was set at 1. Error bars represent mean values (± SD) of two biological replicates.

Figure S3. Effect of ectopic RxLR24 expression on disease resistance of Arabidopsis to *Botrytis cinerea*. Plants were inoculated with *B. cinerea* strain BMM. Diagram shows the diameter of lesions measured 3 dpi. Results represent the mean (± SD) values obtained for 128 leaves in 2 independent experiments. There are no statistically significant differences between group means as determined by one-way ANOVA at the $P<0.05$ level for $F(2) = 0.65$, $P = 0.524$.

Figure S4. High magnification pictures of GFP-RxLR24 positive vesicles. RxLR24 positive vesicles observed under confocal microscope in the cells of transgenic Arabidopsis leaf (upper panel) and root (lower panel). White rectangles mark the fragments which are zoomed in the panel on the right side. The approximate size of vesicles varies from 0.8 to 2 μm. Scale bar represents 2 μm.

Figure S5. RxLR24 accumulates in the membrane fraction. *N. benthamiana* leaves expressing FLAG-RxLR24 or FLAG-RxLR24ΔC, respectively, were used for cell fractionation. Fractions representing 40 mg of leaf tissue were analyzed by SDS-PAGE and immunoblotting with anti-FLAG antibodies. The FLAG-RxLR24 protein accumulated in the membrane fraction (MF). In contrast, the truncated FLAG-RxLR24ΔC was present exclusively in the soluble fraction (SF). Ponceau-S (PS) stained Rubisco large subunit served as a loading control for membrane purity.

Figure S6. Intensity profiles of the co-localization pictures shown in Figure 4b–e. White arrows indicate locations analyzed by fluorescence intensity plots shown in graphs to the right side of each image. The length of the arrows corresponds to the x-axis in the graphs.

Figure S7. Elevated expression level of PR-1, PDF1.2 and PNP-A transcripts observed 24 h after inoculation with *P. brassicae* in Ws-0 wild-type plants. Real time PCR analysis was performed with *expG* as reference transcript. The results represent the mean value (± SD) of two biological replicates.

Figure S8. Effect of RxLR24 on callose deposition in response to *P. brassicae*. Leaves of Arabidopsis wildtype (WT) and different Arabidopsis lines expressing RxLR24 (L1, L2, L3 and L4) were stained 6 hpi for callose accumulation. The Arabidopsis mutant *pmr4* (*powdery mildew resistant 4*) with a defect in pathogen-induced callose production served as a negative control. Scale bar = 100 μm.

Table S1. Sequence comparison of RxLR24 homologs of selected *Phytophthora* species. Percentage of identity (similarity) between RxLR24 protein sequences of five different *Phytophthora* species. Sequences encoding signal peptides were excluded from the

comparison. The compared sequences correspond to the sequences listed in Figure S1.

Table S2. Top target candidates identified by untargeted Co-IP/mass spectrometry. Mass spectrometry data of *Arabidopsis thaliana* proteins with the strongest association to the RxLR24 effector after co-immunoprecipitation. Predicted protein localization based on UniProt database. Peptide spectrum matching results were from Mascot (Matrix Science) searches and only those matching with a probability score > 95% are shown. Numbers reflect the number of total unique peptides matched per protein. In parallel with *Pb*RxLR24, three non-related FLAG-tagged RxLR effectors of *P. brassicae* were used as negative controls. Proteins marked with asterisks were chosen to verify the interaction with the RxLR24 in reciprocal Co-IP experiments. Accession numbers: *Pb*RxLR23 (MG489827), *Pb*RxLR24 (MG489826), *Pb*RxLR27 (MG489828) and *Pb*RxLR29 (MG489829).

Table S3. List of primers used for PCR amplification of cDNAs and plasmids used for the generation of fusion proteins. † Obtained from gene synthesis service (GenScript).

Table S4. List of primers used for qPCR analysis.

File S1. List of peptide sequences derived from proteins associated with *Pb*RxLR24 in Co-IP experiment.

Movie S1. Movement of GFP-RxLR24 positive vesicles in leaf cells. Movie (15 fps) shows vesicle movement observed with confocal microscopy in epidermal leaf cells. The movie consists of 100 time points and was recorded with use of EMCCD camera and 60x magnification. Exposure time was 200 ms.

Movie S2. Movement of GFP-RxLR24 positive vesicles in leaf cells. Movie (15 fps) shows vesicle movement observed with confocal microscopy in the root cells. The movie consists 300 time points and was recorded with use of EMCCD camera and 60x magnification. Exposure time was 500 ms.

REFERENCES

Abas, L. and Luschnig, C. (2010) Maximum yields of microsomal-type membranes from small amounts of plant material without requiring ultracentrifugation. *Analyt. Biochem.* **401**, 217–227.

Anderson, P., Brundrett, M., Grierson, P. and Robinson, R. (2010) Impact of severe forest dieback caused by *Phytophthora cinnamomi* on macrofungal diversity in the northern jarrah forest of Western Australia. *For. Ecol. Manage.* **259**, 1033–1040.

Anderson, R.G., Casady, M.S., Fee, R.A., Vaughan, M.M., Deb, D., Fedkenheuer, K., Huffaker, A., Schmelz, E.A., Tyler, B.M. and McDowell, J.M. (2012) Homologous RXLR effectors from *Hyaloperonospora arabidopsidis* and *Phytophthora sojae* suppress immunity in distantly related plants. *Plant J.* **72**, 882–893.

Anderson, R.G., Deb, D., Fedkenheuer, K. and McDowell, J.M. (2015) Recent progress in RXLR effector research. *Mol. Plant Microbe Interact.* **28**, 1063–1072.

Asaoka, R., Uemura, T., Ito, J., Fujimoto, M., Ito, E., Ueda, T. and Nakano, A. (2013) Arabidopsis RABA1 GTPases are involved in transport between the trans-Golgi network and the plasma membrane, and are required for salinity stress tolerance. *Plant J.* **73**, 240–249.

Bartetzko, V., Sonnewald, S., Vogel, F., Hartner, K., Stadler, R., Hammes, U.Z. and Börnke, F. (2009) The *Xanthomonas campestris* pv. *vesicatoria* type III effector protein XopJ inhibits protein secretion: evidence for interference with cell wall-associated defense responses. *Mol. Plant Microbe Interact.* **22**, 655–664.

Berson, T., Von Wangenheim, D., Takáč, T., Šamajová, O., Rosero, A., Ovečka, M., Komis, G., Stelzer, E.H. and Šamaj, J. (2014) Trans-Golgi network localized small GTPase RabA1d is involved in cell plate formation and oscillatory root hair growth. *BMC Plant Biol.* **14**, 252.

Boevink, P.C., Wang, X., McLellan, H. *et al.* (2016) A *Phytophthora infestans* RXLR effector targets plant PP1c isoforms that promote late blight disease. *Nat. Commun.* **7**, 10311.

Boller, T. and Felix, G. (2009) A renaissance of elicitors: perception of microbe-associated molecular patterns and danger signals by pattern-recognition receptors. *Ann. Rev. Plant Biol.* **60**, 379–406.

Bos, J.I., Armstrong, M.R., Gilroy, E.M. *et al.* (2010) *Phytophthora infestans* effector AVR3a is essential for virulence and manipulates plant immunity by stabilizing host E3 ligase CMPG1. *Proc. Natl Acad. Sci. USA*, **107**, 9909–9914.

Bouwmeester, K., De Sain, M., Weide, R., Gouget, A., Klamer, S., Canut, H. and Govers, F. (2011) The lectin receptor kinase LecRK-I. 9 is a novel *Phytophthora resistance* component and a potential host target for a RXLR effector. *PLoS Pathog.* **7**, e1001327.

Bozkurt, T.O., Schornack, S., Win, J. *et al.* (2011) Phytophthora infestans effector AVRblb2 prevents secretion of a plant immune protease at the haustorial interface. *Proc. Natl Acad. Sci. USA*, **108**, 20832–20837.

Chaparro-Garcia, A., Schwizer, S., Sklenar, J., Yoshida, K., Petre, B., Bos, J.I., Schornack, S., Jones, A.M., Bozkurt, T.O. and Kamoun, S. (2015) *Phytophthora infestans* RXLR-WY effector AVR3a associates with dynamin-related protein 2 required for endocytosis of the plant pattern recognition receptor FLS2. *PLoS ONE*, **10**, e0137071.

Chisholm, S.T., Coaker, G., Day, B. and Staskawicz, B.J. (2006) Host-microbe interactions: shaping the evolution of the plant immune response. *Cell*, **124**, 803–814.

Chow, C.M., Neto, H., Foucart, C. and Moore, I. (2008) Rab-A2 and Rab-A3 GTPases define a trans-golgi endosomal membrane domain in Arabidopsis that contributes substantially to the cell plate. *Plant Cell*, **20**, 101–123.

Clough, S.J. and Bent, A.F. (1998) Floral dip: a simplified method for Agrobacterium-mediated transformation of Arabidopsis thaliana. *Plant J.* **16**, 735–743.

Cooke, D.E., Cano, L.M., Raffaele, S., Bain, R.A., Cooke, L.R., Etherington, G.J., Deahl, K.L., Farrer, R.A., Gilroy, E.M. and Goss, E.M. (2012) Genome analyses of an aggressive and invasive lineage of the Irish potato famine pathogen. *PLoS Pathog.* **8**, e1002940.

Czechowski, T., Stitt, M., Altmann, T., Udvardi, M.K. and Scheible, W.-R. (2005) Genome-wide identification and testing of superior reference genes for transcript normalization in Arabidopsis. *Plant Physiol.* **139**, 5–17.

Dagdas, Y.F., Belhaj, K., Maqbool, A. *et al.* (2016) An effector of the Irish potato famine pathogen antagonizes a host autophagy cargo receptor. *Elife*, **5**, e10856.

Dodds, P.N. and Rathjen, J.P. (2010) Plant immunity: towards an integrated view of plant–pathogen interactions. *Nat. Rev. Genet.* **11**, 539–548.

Dou, D., Kale, S.D., Wang, X., Jiang, R.H., Bruce, N.A., Arredondo, F.D., Zhang, X. and Tyler, B.M. (2008) RXLR-mediated entry of *Phytophthora sojae* effector Avr1b into soybean cells does not require pathogen-encoded machinery. *Plant Cell*, **20**, 1930–1947.

Du, Y., Mpina, M.H., Birch, P.R., Bouwmeester, K. and Govers, F. (2015) *Phytophthora infestans* RXLR effector AVR1 interacts with exocyst component Sec5 to manipulate plant immunity. *Plant Physiol.* **169**, 1975–1990.

Du, Y., Overdijk, E.J.R., Berg, J.A., Govers, F. and Bouwmeester, K. (2018) Solanaceous exocyt subunits are involved in immunity to diverse plant pathogens. *J. Exp. Bot.* **69**, 655–666.

Earley, K.W., Haag, J.R., Pontes, O., Opper, K., Juehne, T., Song, K. and Pikaard, C.S. (2006) Gateway-compatible vectors for plant functional genomics and proteomics. *Plant J.* **45**, 616–629.

Ellinger, D., Glockner, A., Koch, J., Naumann, M., Sturtz, V., Schutt, K., Manisseri, C., Somerville, S.C. and Voigt, C.A. (2014) Interaction of the Arabidopsis GTPase RabA4c with its effector PMR4 results in complete penetration resistance to powdery mildew. *Plant Cell*, **26**, 3185–3200.

Ellis, J.G. and Dodds, P.N. (2011) Showdown at the RXLR motif: serious differences of opinion in how effector proteins from filamentous eukaryotic pathogens enter plant cells. *Proc. Natl Acad. Sci. USA*, **108**, 14381–14382.

Feraru, E., Feraru, M.I., Asaoka, R., Paciorek, T., De Rycke, R., Tanaka, H., Nakano, A. and Friml, J. (2012) BEX5/RabA1b regulates trans-Golgi network-to-plasma membrane protein trafficking in Arabidopsis. *Plant Cell*, **24**, 3074–3086.

Frei dit Frey, N. and Robatzek, S. (2009) Trafficking vesicles: pro or contra pathogens? *Curr. Opin. Plant Biol.* **12**, 437–443.

Haas, B.J., Kamoun, S., Zody, M.C., Jiang, R.H., Handsaker, R.E., Cano, L.M., Grabherr, M., Kodira, C.D., Raffaele, S. and Torto-Alalibo, T. (2009)

Genome sequence and analysis of the Irish potato famine pathogen *Phytophthora infestans*. *Nature*, **461**, 393–398.

Haverkort, A., Struik, P., Visser, R. and Jacobsen, E. (2009) Applied biotechnology to combat late blight in potato caused by *Phytophthora infestans*. *Potato Res.* **52**, 249–264.

Hutagalung, A.H. and Novick, P.J. (2011) Role of Rab GTPases in membrane traffic and cell physiology. *Physiol. Rev.* **91**, 119–149.

Inada, N. and Ueda, T. (2014) Membrane trafficking pathways and their roles in plant-microbe interactions. *Plant Cell Physiol.* **55**, 672–686.

Jing, M., Guo, B., Li, H., Yang, B., Wang, H., Kong, G., Zhao, Y., Xu, H., Wang, Y. and Ye, W. (2016) A *Phytophthora sojae* effector suppresses endoplasmic reticulum stress-mediated immunity by stabilizing plant binding immunoglobulin proteins. *Nat. Commun.* **7**, 11685.

Jones, J.D. and Dangl, J.L. (2006) The plant immune system. *Nature*, **444**, 323–329.

Kale, S.D. (2012) Oomycete and fungal effector entry, a microbial Trojan horse. *New Phytol.* **193**, 874–881.

Karimi, M., Inzé, D. and Depicker, A. (2002) GATEWAY™ vectors for Agrobacterium-mediated plant transformation. *Trends Plant Sci.* **7**, 193–195.

King, S.R., McLellan, H., Boevink, P.C., Armstrong, M.R., Bukharova, T., Sukarta, O., Win, J., Kamoun, S., Birch, P.R. and Banfield, M.J. (2014) *Phytophthora infestans* RXLR effector PexRD2 interacts with host MAPKKK epsilon to suppress plant immune signaling. *Plant Cell*, **26**, 1345–1359.

Koch, E. and Slusarenko, A. (1990) Arabidopsis is susceptible to infection by a downy mildew fungus. *Plant Cell*, **2**, 437–445.

Kwon, C., Bednarek, P. and Schulze-Lefert, P. (2008) Secretory pathways in plant immune responses. *Plant Physiol.* **147**, 1575–1583.

Le Fevre, R., Evangelisti, E., Rey, T. and Schornack, S. (2015) Modulation of host cell biology by plant pathogenic microbes. *Annu. Rev. Cell Dev. Biol.* **31**, 201–229.

L'Haridon, F., Besson-Bard, A., Binda, M. *et al.* (2011) A permeable cuticle is associated with the release of reactive oxygen species and induction of innate immunity. *PLoS Pathog.* **7**, e1002148.

Lunn, D., Gaddipati, S.R., Tucker, G.A. and Lycett, G.W. (2013) Null mutants of individual RABA genes impact the proportion of different cell wall components in stem tissue of Arabidopsis thaliana. *PLoS ONE*, **8**, e75724.

McLellan, H., Boevink, P.C., Armstrong, M.R., Pritchard, L., Gomez, S., Morales, J., Whisson, S.C., Beynon, J.L. and Birch, P.R. (2013) An RxLR effector from *Phytophthora infestans* prevents re-localisation of two plant NAC transcription factors from the endoplasmic reticulum to the nucleus. *PLoS Pathog.* **9**, e1003670.

Nomura, K., DebRoy, S., Lee, Y.H., Pumplin, N., Jones, J. and He, S.Y. (2006) A bacterial virulence protein suppresses host innate immunity to cause plant disease. *Science*, **313**, 220–223.

Nomura, K., Mecey, C., Lee, Y.-N., Imboden, L.A., Chang, J.H. and He, S.Y. (2011) Effector-triggered immunity blocks pathogen degradation of an immunity-associated vesicle traffic regulator in Arabidopsis. *Proc. Natl Acad. Sci. USA*, **108**, 10774–10779.

Qi, X. and Zheng, H. (2013) Rab-A1c GTPase defines a population of the trans-Golgi network that is sensitive to endosidin1 during cytokinesis in Arabidopsis. *Mol. Plant*, **6**, 847–859.

Qiao, Y., Shi, J., Zhai, Y., Hou, Y. and Ma, W. (2015) Phytophthora effector targets a novel component of small RNA pathway in plants to promote infection. *Proc. Natl Acad. Sci. USA*, **112**, 5850–5855.

Rafiqi, M., Ellis, J.G., Ludowici, V.A., Hardham, A.R. and Dodds, P.N. (2012) Challenges and progress towards understanding the role of effectors in plant–fungal interactions. *Curr. Opin. Plant Biol.* **15**, 477–482.

Rehman, R.U., Stigliano, E., Lycett, G.W., Sticher, L., Sbano, F., Faraco, M., Dalessandro, G. and Di Sansebastiano, G.P. (2008) Tomato Rab11a characterization evidenced a difference between SYP121-dependent and SYP122-dependent exocytosis. *Plant Cell Physiol.* **49**, 751–766.

Rigal, A., Doyle, S.M. and Robert, S. (2015) Live cell imaging of FM4-64, a tool for tracing the endocytic pathways in Arabidopsis root cells. In *Plant Cell Expansion: Methods and Protocols* (Estevez, J.M., ed.). Springer, pp. 93–103.

Roetschi, A., Si-Ammour, A., Belbahri, L., Mauch, F. and Mauch-Mani, B. (2001) Characterization of an Arabidopsis-Phytophthora pathosystem: resistance requires a functional PAD2 gene and is independent of salicylic acid, ethylene and jasmonic acid signalling. *Plant J.* **28**, 293–305.

Saunders, D.G., Breen, S., Win, J. *et al.* (2012) Host protein BSL1 associates with *Phytophthora infestans* RXLR effector AVR2 and the *Solanum demissum* immune receptor R2 to mediate disease resistance. *Plant Cell*, **24**, 3420–3434.

Schlaeppi, K., Abou-Mansour, E., Buchala, A. and Mauch, F. (2010) Disease resistance of Arabidopsis to Phytophthora brassicae is established by the sequential action of indole glucosinolates and camalexin. *Plant J.* **62**, 840–851.

Schmidt, S.M., Kuhn, H., Micali, C., Liller, C., Kwaaitaal, M. and Panstruga, R. (2014) Interaction of a *Blumeria graminis* f. sp. *hordei* effector candidate with a barley ARF-GAP suggests that host vesicle trafficking is a fungal pathogenicity target. *Mol. Plant Pathol.* **15**, 535–549.

Schulze, S., Kay, S., Büttner, D., Egler, M., Eschen-Lippold, L., Hause, G., Krüger, A., Lee, J., Müller, O. and Scheel, D. (2012) Analysis of new type III effectors from *Xanthomonas* uncovers XopB and XopS as suppressors of plant immunity. *New Phytol.* **195**, 894–911.

Schütze, K., Harter, K. and Chaban, C. (2009) Bimolecular fluorescence complementation (BiFC) to study protein-protein interactions in living plant cells. In *Plant Signal Transduction: Methods and Protocols* (Botella, J.R. and Botella, M.R. eds). Totowa NJ: Humana Press, pp. 189–202.

Shandala, T., Woodcock, J.M., Ng, Y., Biggs, L., Skoulakis, E.M., Brooks, D.A. and Lopez, A.F. (2011) Drosophila 14-3-3ε has a crucial role in antimicrobial peptide secretion and innate immunity. *J. Cell Sci.* **124**, 2165–2174.

Shimada, T.L., Shimada, T. and Hara-Nishimura, I. (2010) A rapid and non-destructive screenable marker, FAST, for identifying transformed seeds of Arabidopsis thaliana. *Plant J.* **61**, 519–528.

Stenmark, H. (2009) Rab GTPases as coordinators of vesicle traffic. *Nat. Rev. Mol. Cell Biol.* **10**, 513–525.

Szumlanski, A.L. and Nielsen, E. (2009) The Rab GTPase RabA4d regulates pollen tube tip growth in *Arabidopsis thaliana*. *Plant Cell*, **21**, 526–544.

Takken, F. and Tameling, W. (2009) To nibble at plant resistance proteins. *Science*, **324**, 744–746.

Thomma, B.P., Cammune, B. and Thevissen, K. (2002) Plant defensins. *Planta*, **216**, 193–202.

Ton, J. and Mauch-Mani, B. (2004) β-Amino-butyric acid-induced resistance against necrotrophic pathogens is based on ABA-dependent priming for callose. *Plant J.* **38**, 119–130.

Tyler, B.M., Tripathy, S., Zhang, X., Dehal, P., Jiang, R.H., Aerts, A., Arredondo, F.D., Baxter, L., Bensasson, D. and Beynon, J.L. (2006) Phytophthora genome sequences uncover evolutionary origins and mechanisms of pathogenesis. *Science*, **313**, 1261–1266.

Van Loon, L.C. and Van Strien, E.A. (1999) The families of pathogenesis-related proteins, their activities, and comparative analysis of PR-1 type proteins. *Physiol. Mol. Plant Pathol.* **55**, 85–97.

Vandesompele, J., De Preter, K., Pattyn, F., Poppe, B., Van Roy, N., De Paepe, A. and Speleman, F. (2002) Accurate normalization of real-time quantitative RT-PCR data by geometric averaging of multiple internal control genes. *Gen. Biol.* **3**, research0034.1–research0034.11.

Vernoud, V., Horton, A.C., Yang, Z. and Nielsen, E. (2003) Analysis of the small GTPase gene superfamily of Arabidopsis. *Plant Physiol.* **131**, 1191–1208.

Wang, D., Weaver, N.D., Kesarwani, M. and Dong, X. (2005) Induction of protein secretory pathway is required for systemic acquired resistance. *Science*, **308**, 1036–1040.

Wang, Q., Han, C., Ferreira, A.O., Yu, X., Ye, W., Tripathy, S., Kale, S.D., Gu, B., Sheng, Y. and Sui, Y. (2011a) Transcriptional programming and functional interactions within the *Phytophthora sojae* RXLR effector repertoire. *Plant Cell*, **23**, 2064–2086.

Wang, Y.H., Gehring, C. and Irving, H.R. (2011b) Plant natriuretic peptides are apoplastic and paracrine stress response molecules. *Plant Cell Physiol.* **52**, 837–850.

Wang, X., Boevink, P., McLellan, H., Armstrong, M., Bukharova, T., Qin, Z. and Birch, P.R. (2015) A host KH RNA-binding protein is a susceptibility factor targeted by an RXLR effector to promote late blight disease. *Mol. Plant*, **8**, 1385–1395.

Wang, W.M., Liu, P.Q., Xu, Y.J. and Xiao, S. (2016) Protein trafficking during plant innate immunity. *J. Integr. Plant Biol.* **58**, 284–298.

Wawra, S., Djamei, A., Albert, I., Nurnberger, T., Kahmann, R. and van West, P. (2013) In vitro translocation experiments with RxLR-reporter fusion proteins of Avr1b from *Phytophthora sojae* and AVR3a from *Phytophthora infestans* fail to demonstrate specific autonomous uptake in plant and animal cells. *Mol. Plant Microbe Interact.* **26**, 528–536.

Whisson, S.C., Boevink, P.C., Moleleki, L., Avrova, A.O., Morales, J.G., Gilroy, E.M., Armstrong, M.R., Grouffaud, S., Van West, P. and Chapman, S. (2007) A translocation signal for delivery of oomycete effector proteins into host plant cells. *Nature*, **450**, 115–118.

Yaeno, T. and Shirasu, K. (2013) The RXLR motif of oomycete effectors is not a sufficient element for binding to phosphatidylinositol monophosphates. *Plant Signal. Behav.* **8**, e23865.

Yang, L., McLellan, H., Naqvi, S. *et al.* (2016) Potato NPH3/RPT2-like protein StNRL1, targeted by a *Phytophthora infestans* RXLR effector, is a susceptibility factor. *Plant Physiol.* **171**, 645–657.

Zavaliev, R. and Epel, B.L. (2015) Imaging callose at plasmodesmata using aniline blue: quantitative confocal microscopy. *Methods Mol. Biol.* **1217**, 105–119.

Zheng, H., Camacho, L., Wee, E., Batoko, H., Legen, J., Leaver, C.J., Malho, R., Hussey, P.J. and Moore, I. (2005) A Rab-E GTPase mutant acts downstream of the Rab-D subclass in biosynthetic membrane traffic to the plasma membrane in tobacco leaf epidermis. *Plant Cell*, **17**, 2020–2036.

Zipfel, C. (2014) Plant pattern-recognition receptors. *Trends Immunol.* **35**, 345–351.